論文 / 著書情報
Article / Book Information

Title	Self-Holding Magneto-Optical Switch Integrated with Thin-Film Magnet
Authors	K. Okazeri, K. Muraoka, Y. Shoji, S. Nakagawa, N. Nishiyama, S. Arai, T. Mizumoto
Citation	IEEE Photonics Technol. Lett., vol. 30, no. 4, pp. 371-374
Pub. date	2018, 1
Copyright	(c) 2018 IEEE. Personal use of this material is permitted. Permission from IEEE must be obtained for all other uses, in any current or future media, including reprinting/republishing this material for advertising or promotional purposes, creating new collective works, for resale or redistribution to servers or lists, or reuse of any copyrighted component of this work in other works.
DOI	http://dx.doi.org/10.1109/LPT.2018.2791924
Note	This file is author (final) version.

Self-Holding Magneto-Optical Switch Integrated with Thin-Film Magnet

Ken Okazeri, Kenji Muraoka, Yuya Shoji, *Member, IEEE*, Shigeki Nakagawa, *Member, IEEE*, Nobuhiko Nishiyama, *Senior Member, IEEE*, Shigehisa Arai, *Fellow, IEEE*, and Tetsuya Mizumoto, *Fellow, IEEE*

***Abstract*—We demonstrate a novel self-holding function of a magneto-optical waveguide switch. The switching state is flipped by a pulsed current and maintained without any power supply by virtue of the non-volatility of the thin-film magnet. Extinction ratios up to 15.4 dB were demonstrated. The switch state was controlled by a 1-μs pulsed electrical current.**

***Index Terms*—Optical switches, Optical waveguides, Magnetooptic devices, Magnetooptic effects.**

I. Introduction

GROWTH of smartphones, movie streaming, and cloud services significantly increases internet traffic. Photonic network systems have been developed to support a large amount of traffic, and to increase capacity and reduce power consumption. Conventional approaches to increasing symbol rate and number of wavelength channels reach the fundamental limits of Shannon's theorem and fiber fuse. Thus, flexible and efficient optical path networking methods such as applying optical cross-connect systems have been intensively investigated [1,2]. Optical switches become more important where small size and low power consumption, rather than high-speed operation are required. Current-driven optical switches are realized with a small footprint using the thermo-optic effect and carrier injection in semiconductors. However, these switches consume a great deal of power to maintain the switch state [3–6]. Although voltage-driven optical switches can operate with low power consumption, mirror-switch-based micro electro mechanical systems with free-space optics and electro-optical switches based on lithium niobate have large device size [7,8].

In this paper, we propose a novel magneto-optical (MO) switch with self-holding operation, for which we define the switch state to be maintained without any power supply. Such optical switches have been reported with a phase-change material [9] and floating gate transistor waveguide [10]. However, they have fundamental limitation of rewriting times. Proposed optical switching is realized using the MO effect of the MO garnet, combined with thin-film magnets whose magnetization is controlled by a pulsed current. There is no limitation of rewriting times in magnetization only controlled by the magnetic field without heating. Ultra-low power consumption is possible in network systems with relatively low switching frequency. Additionally, small footprints can be expected when using silicon photonic waveguides.

II. Self-Holding Magneto-Optical Switch

A. Device Structure

Figure 1(a) shows the schematic of the proposed MO switch. Hydrogenated amorphous silicon (a-Si:H) and cerium-substituted yttrium iron garnet (Ce:YIG) are used as core and under-cladding layers, respectively. Thin-film magnets of FeCoB and silver electrodes are formed above the waveguide on a SiO_2 over-cladding layer. The device consists of a Mach–Zehnder interferometer (MZI) composed of two 3-dB directional couplers, a path length phase shifter, and MO phase shifters. The 3-dB directional couplers split the input light wave at equal amplitudes into the two interferometer waveguide arms. The path length phase shifter gives $+\pi/2$ phase difference between the two arms. The MO phase shifters give a phase difference between the two arms based on a transverse MO Kerr effect in the lower cladding layer of Ce:YIG with magnetizations aligned in anti-parallel directions. A magnetic field is applied to the Ce:YIG by the residual magnetization of the thin-film magnets. When the applied magnetic field is directed inward, the MO phase shifters provide a $-\pi/2$ phase difference. As a result, the total phase difference becomes 0 and the light wave is output at the cross port. When the applied magnetic field is directed outward, the phase difference provided by the MO effect becomes $+\pi/2$. Thus, the total phase difference amounts to π and the light wave is output at the bar port.

The magnetization of the thin-film magnet is controlled by a current flow in the silver electrode. The current flow induces a

Manuscript received *** **, 2017; revised *** **, 2017; accepted *** **, 2017. Date of publication *** **, 2017. This work was supported by the JST Core Research for Evolutional Science and Technology (CREST) #JPMJCR15N6; the MIC/SCOPE #162103103; the JSPS KAKENHI in Japan under Grant 16K06295; and the TEPCO Memorial Foundation.

K. Okazeri, K. Muraoka, S. Nakagawa, N. Nishiyama, and T. Mizumoto are with the Department of Electrical and Electronic Engineering, Tokyo Institute of Technology, Tokyo, 152-8552 Japan. (e-mail: okazeri.k.aa @m.titech.ac.jp, muraoka.k.ac@m.titech.ac.jp, nakagawa@ee.e.titech.ac.jp, nishiyama@ee.e.titech.ac.jp, tmizumot@pe.titech.ac.jp).

Y. Shoji and S. Arai were with the Laboratory for Future Interdisciplinary Research of Science and Technology (FIRST), Tokyo Institute of Technology, Tokyo, 152-8552 Japan (e-mail: shoji@ee.e.titech.ac.jp, arai@pe.titech.ac.jp).

circular magnetic field around the electrode, as shown in Fig. 1(b), which magnetizes the thin-film magnet along the magnetic field direction. The switching state is maintained by the residual magnetization of the thin film magnets, as shown in Fig. 1(c). The electrode is patterned so as to induce a magnetic field in the anti-parallel direction in the two MZI arms. The current can be a short pulse, but one that is sufficient to flip the magnetization of the thin-film magnet.

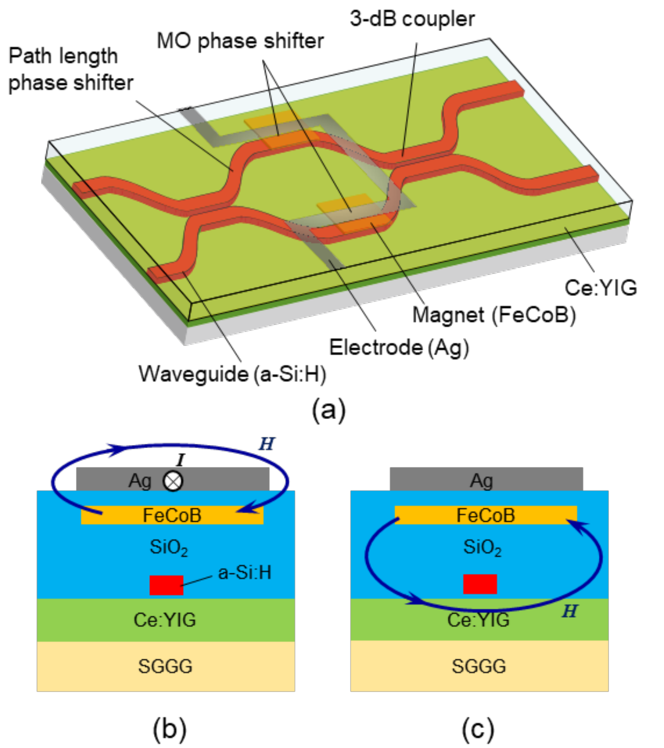

Fig. 1. (a) Configuration of proposed magneto-optical switch. (b) Changing switching state via current flow. (c) Maintaining switching state because of non-volatility of thin-film magnet.

B. Magnet Design

The thin-film magnet maintains the switching state in the MO phase shifters. The magnet should have not only a strong magnetization but also a relatively low coercive force, because the magnetization is flipped by a current-induced magnetic field. Here, we employ a soft magnetic material FeCoB [11]. Magnets are patterned as an array of strips above the waveguide, as shown in Fig. 2. The long axis of each strip is set to be orthogonal to the waveguide because the magnetization of the magnet is easily aligned with the long axis because of shape anisotropy. Figure 3 shows the magnetization characteristics of Ce:YIG. When a magnetic field over 50 Oe is applied to the Ce:YIG, the magnetization is saturated. Therefore, the residual magnetization of the thin-film magnets has to be strong enough to induce the magnetic field. We designed the dimensions of the magnet strips as follows: long and short axis lengths, height, and distance between magnets were 20 μm, 5 μm, 150 nm, and 3 μm, respectively. Figure 4 shows the measured magnetization characteristics of the FeCoB magnet array fabricated using a facing-target sputtering method [12]. The blue and red lines show the magnetization characteristics of the easy and hard axis directions, respectively. These lines indicate that the magnets are magnetically anisotropic. The residual magnetization of the easy axis is 12.5 kG. We calculated that the magnets can give magnetic field of 38.5 Oe in the Ce:YIG layer with a distance of 1 μm, which is necessary to avoid optical absorption by the thin-film magnet. This value is not sufficient to saturate the Ce:YIG, and results in insufficient MO phase shifting, as described in the measurements for the optical switch.

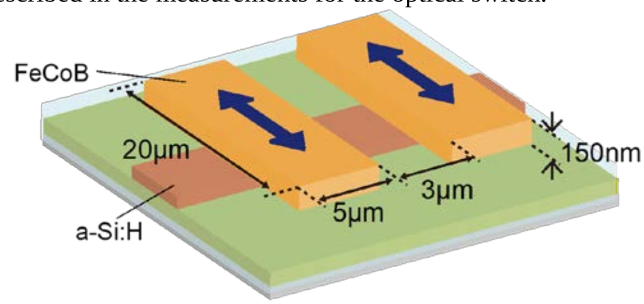

Fig. 2. Design of thin-film magnets.

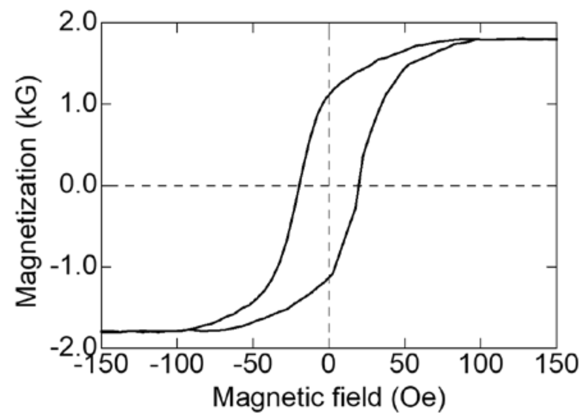

Fig. 3. Hysteresis loop of Ce:YIG.

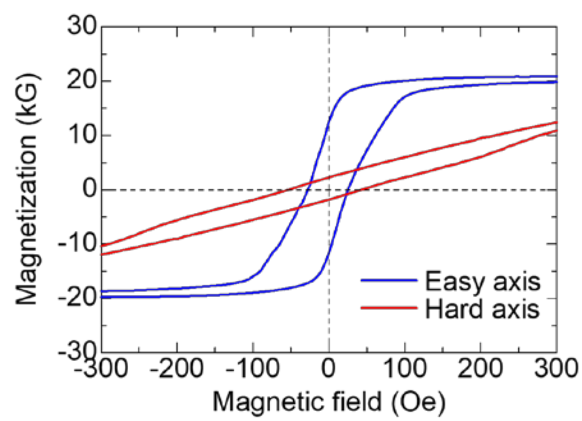

Fig. 4. Hysteresis loops of 20 μm × 5 μm strip array of FeCoB.

C. Fabrication

A 500-nm-thick single-crystalline Ce:YIG layer was grown by an RF sputtering on a (Ca, Mg, Zr)-substituted gadolinium gallium garnet (SGGG) substrate. A 30-nm-thick SiO_2 layer was deposited on the Ce:YIG using plasma-enhanced chemical vapor deposition (PCVD) with tetraethyl-orthosilicate gas [13]. Then, a-Si:H layer was deposited using PCVD with SiH_4 gas. An a-Si:H waveguide pattern was formed using electron beam lithography and successive reactive ion etching with CF_4, O_2, and SF_6 gases. The waveguide height and width were 240 nm and 600 nm, respectively. An 800-nm-thick SiO_2 over-cladding layer was deposited. Next, 150-nm-thick FeCoB was deposited with a 10-nm-thick Ru buffer layer using an RF facing-targets sputtering method. The magnet was patterned using a lift-off process. After a 150-nm-thick SiO_2 cover layer was deposited, a 30-µm-wide and 500-nm-thick silver electrode was deposited and formed using an evaporation process and a lift-off process.

Figure 5 shows a microscope image of the fabricated optical switch. Thin-film magnets are patterned as an array of 20 µm × 5 µm strips. Although the required length of an MO phase shifter for providing $\pm\pi/2$ phase difference was calculated to be ~500 µm [14], the longer length of 745 µm was used to operate the MO switch based on the unsaturated magnetization of Ce:YIG. The path length phase shifter was 13.58-µm-long, which provided $\pi/2+40\pi$ so that some extinction peaks could be observed in the measurable wavelength range.

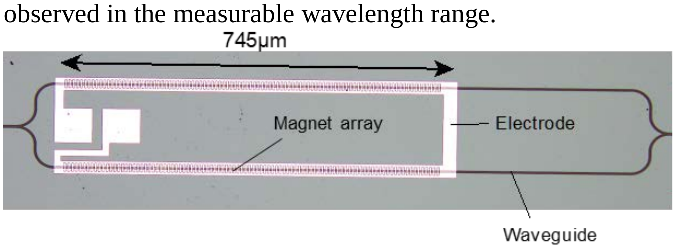

Fig. 5. Microscope image of fabricated MO switch.

III. Results and Discussion

A. Spectral Characteristics

First, we measured the wavelength characteristics of the fabricated device in a static manner. Figure 6 shows our experimental setup. The MO switch operates in the transverse magnetic (TM) mode of light because the MO phase shift is provided only in the TM mode. Light from an amplified spontaneous emission source was polarized to the TM mode and launched to the device under test. The output spectrum was measured using a spectrum analyzer. The electric current was injected and controlled by a variable voltage source via two micro-probes attached to the electrode. We applied a current ~200 mA to the electrode for 1 s to magnetize the thin-film magnet array. Several seconds after ceasing the current, we measured the transmission spectrum. Then, we applied a current in the opposite direction to flip the magnetization. Several seconds after ceasing the current, we measured the transmission spectrum again.

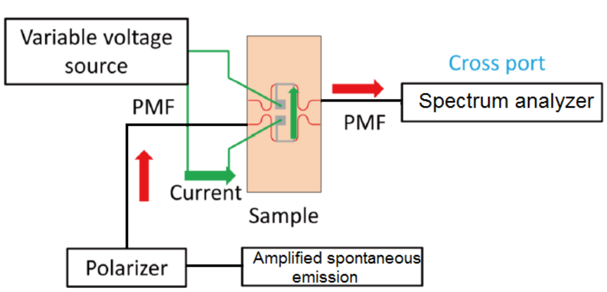

Fig. 6. Experimental setup for measuring wavelength characteristics.

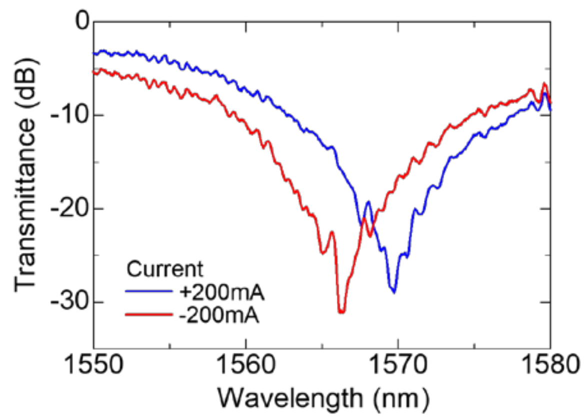

Fig. 7. Measured transmission spectra of MO switch several seconds after ceasing the current.

Figure 7 shows the transmission spectra measured at the cross port for each magnetization direction after applying a current. Different optical transmittances were observed when flipping the magnetization direction. Results indicated that the switch state was changed by the applied current. A maximum extinction ratio of 15.4 dB was obtained at a wavelength of 1566 nm. Ideally, the maximum transmission is obtained for one state at the wavelength at which the other state shows minimum transmission. The measured result indicates that the obtained phase shift in the MZI was ~0.15π, which is less than the designed value of $\pi/2$. This difference can be attributed both to residual magnetization of the thin-film magnet that is insufficient to saturate Ce:YIG and to insufficient MO phase shift due to dimensional errors in the waveguide structure. For example, the MO phase shift is decreased when the thickness of a-Si core or SiO_2 interlayer between a-Si and Ce:YIG is larger than the designed value. We believe these problems can be solved by improving the magnetic characteristics of the FeCoB and optimizing the structural design.

B. Pulse Response

We measured the temporal response of the device under pulsed-current driving. Figure 8 shows the experimental setup. Light from a tunable laser at a wavelength of 1562 nm was launched to the device under test. A pulse voltage of ±2 V amplitude and 1-µs width was applied to the electrode of the device at a repetition rate of 10 kHz by a function generator. The output light at the cross port was detected by a photodiode with an electrical gain amplifier; the temporal response was measured using an oscilloscope. The current was estimated to be 200 mA from the applied voltage and the measured DC resistance of electrode 10 Ω. Although the maximum extinction was obtained at wavelengths of 1567 nm and 1570 nm as observed in Fig. 7, the transmitted power was too low to measure the temporal response with our photodiode at the wavelengths. Figure 9 shows the measured results. We observed that the switch state was changed by applying the pulsed voltage and maintained after the voltage became zero. Because of the impedance mismatch of the electrodes, slight overshoot and undershoot of the applied voltage occurred. The spike response of the optical output was caused by the magnetic field generated by the current flowing in the electrode, which also affected the magnetization of the Ce:YIG layer. The slow tail of ~100 μs after the spike was due to the electrical response of the gain amplifier in the photodiode used to compensate for weak optical output. The impedance mismatch caused insufficient current flowing into the device electrode, which resulted in less MO phase shift than that induced by a DC current. Although the extinction ratio was insufficient at this moment due to the choice of input light wavelength, the self-holding switching operation was successfully confirmed based on the stable output level after the transient response. We believe that this extinction ratio can be improved by adjusting the impedance of the electrode so as to match with high-frequency system as well as reducing dimensional errors.

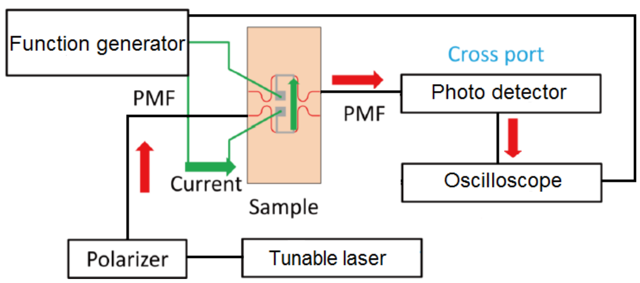

Fig. 8. Experimental setup for measuring temporal response.

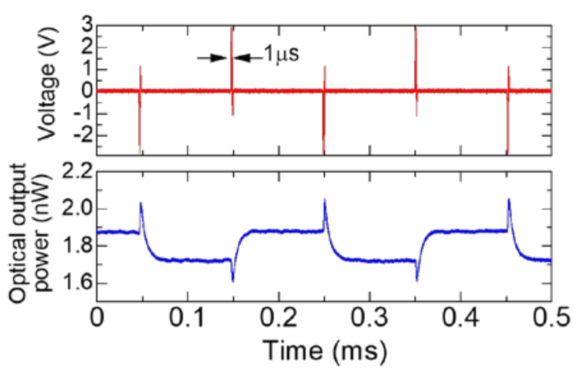

Fig. 9. Measured temporal response of MO switch to a pulsed current.

IV. Conclusion

We demonstrated a novel self-holding function of the MO waveguide switch. The switch state was determined by the sign of the MO effect, which was maintained by the residual magnetization of the thin-film magnet and controlled by the magnetic field induced by the electrical current. Extinction ratios up to 15.4 dB were demonstrated. Additionally, the switch state was maintained after switching by a 1-μs pulsed electrical current.

References

[1] K. Ishii, J. Kurumida, K. Sato, T. Kudoh, and S. Namiki, "Unifying Top-Down and Bottom-Up Approaches to Evaluate Network Energy Consumption," *J. Lightw. Technol.*, vol. 33, no. 21, pp. 4395–4405, 2015.

[2] M. Jinno, H. Takara, Y. Sone, K. Yonenaga, and A. Hirao, "Elastic Optical Path Network Architecture: Framework for spectrally-efficient and scalable future optical networks," *IEICE Trans. Commun.*, vol. E95-B, no. 3, pp. 706–713, 2012.

[3] K. Tanizawa, et al., "Ultra-compact 32x32 Strictly-non-blocking Si-wire Optical Switch with Fan-out LGA Interposer," *Opt. Express*, vol. 23, pp. 17599–17606, 2015.

[4] S. Sohma, T. Watanabe, N. Ooba, M. Itoh, T. Shibata, and H. Takahashi, "Silica-based PLC Type 32x32 Optical Matrix Switch," in *European Conference on Optical Communication*, Cannes, 2006, pp. 24–28.

[5] M.-J. Kwack, T. Tanemura, A. Higo, and Y. Nakano, "Monolithic InP Strictly Non-blocking 8×8 Switch for High Speed WDM Optical Interconnection," *Opt. Express*, vol. 20, pp. 28734–28741, 2012.

[6] M. Yang, W. M. J. Green, S. Assefa, J. V. Campenhout, B. G. Lee, C. V. Jahnes, F. E. Doany, C. L. Schow, J. A. Kash, and Y. A. Vlasov, "Non-Blocking 4x4 Electro-Optic Silicon Switch for On-Chip Photonic Network," *Opt. Express*, vol. 19, no. 1, pp. 47–54, 2010.

[7] T. J. Seok, N. Quack, S. Han, and M. C. Wu, "50x50 Digital Silicon Photonic Switches with MEMS-Actuated Adiabatic Couplers," in *Optical Fiber Communication Conference*, Los Angeles, CA, 2015, paper M2B.4.

[8] T. Kawanishi, T. Sakamoto, M. Tsuchiya, M. Izutsu, S. Mori, and K. Higuma, "70dB Extinction-Ratio LiNbO3 Optical Intensity Modulator for Two-Tone Lightwave Generation," in *Optical Fiber Communication Conference*, Anaheim, CA, 2006, paper OWC4.

[9] D. Tanaka, Y. Shoji, M. Kuwahara, X. Wang, K. Kintaka, H. Kawashima, T. Toyosaki, Y. Ikuma, and H. Tsuda, "Ultra-small, Self-holding, Optical Gate Switch using $Ge_2Sb_2Te_5$ with a Multi-mode Si Waveguide," *Opt. Express*, vol. 20, no. 9, pp. 10283–10294, 2012.

[10] J.-F Song, A. E.-J. Lim, X.-S. Luo, Q. Fang, C. Li, L. X. Jia, X.-G Tu, Y. Huang, H.-F. Zhou, T.-Y. Liow, and G.-Q. Lo, "Silicon Photonic Integrated Circuits with Electrically Programmable Non-volatile Memory Functions," *Opt. Express*, vol. 24, no. 19, pp. 21744–21751, 2016.

[11] M. Munakata, S. Aoqui, and M. Yagi, "B-Concentration Dependence on Anisotropy Field of CoFeB Thin Film for Gigahertz Frequency Use," *IEEE Trans. Magn.*, vol. 41, no. 10, pp. 3262–3264, 2005.

[12] A. Hashimoto, K. Hirata, T. Matsuu, S. Saito, and S. Nakagawa, "Crystal Structure as an Origin of High-Anisotropy Field of FeCoB Films With Ru Underlayer," *IEEE Trans. Magn.*, vol. 44, no. 11, pp. 3899–3901, 2008.

[13] J. Kang, Y. Atsumi, M. Oda, T. Amemiya, N. Nishiyama, and S. Arai, "Low-Loss Amorphous Silicon Multilayer Waveguides Vertically Stacked on Silicon-on-Insulator Substrate," *Jpn. J. Appl. Phys.*, vol. 50, p. 120208, 2011.

[14] E. Ishida, K. Miura, Y. Shoji, T. Mizumoto, N. Nishiyama, and S. Arai, "Magneto-optical Switch with Amorphous Silicon Waveguides on Magneto-optical Garnet," *Jpn. J. Appl. Phys.*, vol. 55, p. 088002, 2016.